How to cite: *Angew. Chem. Int. Ed.* **2024**, *63*, e202412020
doi.org/10.1002/anie.202412020

Supramolecular Chemistry

Mutualistic Synthesis from Orthogonal Dynamic Covalent Reactions

*Yonglei Lyu, Ying Hu, Jinghui Yang, Xin Wang, and Jianwei Li**

Abstract: Mutualisms are interactions that benefit all species involved. It has been widely investigated in neighbouring subjects, such as biology, ecology, sociology, and economics. However, such a reciprocal relationship in synthetic chemical systems has rarely been studied. Here, we demonstrate a mutualistic synthesis where byproducts from two orthogonal chemical reactions aid each other's production. Disulfide exchange and hydrazone exchange were chosen to generate two dynamic combinatorial libraries. A minor tetrameric macrocycle from the active disulfide library was quantitatively amplified in the presence of the hydrazone library. This incorporation also turned on the previously inert hydrazone reaction, producing a linear species that formed a "handcuffs" catenane with the disulfide tetramer. These findings not only lend robust support to the hypothesis of "RNA-peptide coevolution" for the origin of life but also broaden the scope of synthetic chemistry, highlighting the untapped potential of minor products from different reactions. Additionally, the co-self-assembly of these mutualistic entities to form supramolecular structures opens new avenues for future development of composite nanosystems with synergistic properties.

Mutualisms are interactions that benefit all species involved.[1] A typical example of mutualism in ecosystems is the mycorrhizal interaction. Plants produce carbohydrates that support the growth of fungi, while fungi enhance the ability of plant roots to absorb nutrients and water from the soil.[2] This concept has been extensively studied in various fields, such as biology,[3] ecology,[4] sociology,[5] and economics.[6] Mutualism can exist in biochemical systems.[7] When the products of two reactions mutually benefit each other's synthesis, their relationship can be described as mutualistic. However, such positive cooperation in synthetic chemical systems has rarely been explored. Traditionally, chemists have focused on single reactions or sequential reactions, aiming to achieve high yields of target products by optimizing reaction conditions and developing efficient catalysts. Consequently, there has been limited investigation into reciprocal synthesis in complex chemical systems.

Here, we demonstrate the concept of mutualistic synthesis showing that two byproducts from two respective orthogonal chemical reactions could positively cooperate and become dominant when these two reactions take place in the same vial using the tool of dynamic combinatorial chemistry (DCC).[8] During the past two decades, DCC has been a well-established method for studying molecular complexity.[9] It deals with dynamic combinatorial libraries (DCLs), which are produced in a combinatorial way by linking building blocks through reversible chemical reactions. The concentration distribution of library members is typically under thermodynamic control. One strategy to show the principle governed by thermodynamics is introducing external template molecules into a DCL. If the template can lower the energy level of some library members through noncovalent binding, the equilibrium will be shifted by amplifying their concentration while consuming the free species, presenting a competitive molecular behavior inside the DCL.[9b,d–f] Such a "survival of the fittest" presentation allows DCLs to mimic natural selection in molecular systems.

In this work, instead of showing the competition among internal species from the same library, we report the cooperative synthesis of species from different libraries. Specifically, we created two DCLs using two orthogonal reversible chemical reactions, respectively (Figure 1a–b). When these two libraries were performed together at the same experimental condition, two network species that were minor products from the respective DCLs became the major products due to the reduction in Gibbs energy levels arising from the formation of a complex. These results suggested that the two species functioned as templates for each other's co-amplification through noncovalent binding between different libraries, demonstrating a mutualistic relationship in synthesis. Moreover, the inert reaction could be powered on by another active reaction in the pair of orthogonal reactions. Such a reciprocal synthesis stands for a way of coevolution of species in complex chemical systems, shedding some light on the hypothesis of "RNA-peptide

[*] Y. Lyu, J. Yang, X. Wang, Dr. J. Li
MediCity Research Laboratory
University of Turku
Tykistökatu 6, 20520 Turku (Finland)
E-mail: jianwei.li@utu.fi
Y. Lyu, J. Yang, X. Wang
Department of Chemistry
University of Turku
Henrikinkatu 2, Aurum, 20500 Turku (Finland)
Dr. Y. Hu
Department of Chemistry
China Pharmaceutical University
Nanjing 211198, Jiangsu province (P. R. China)

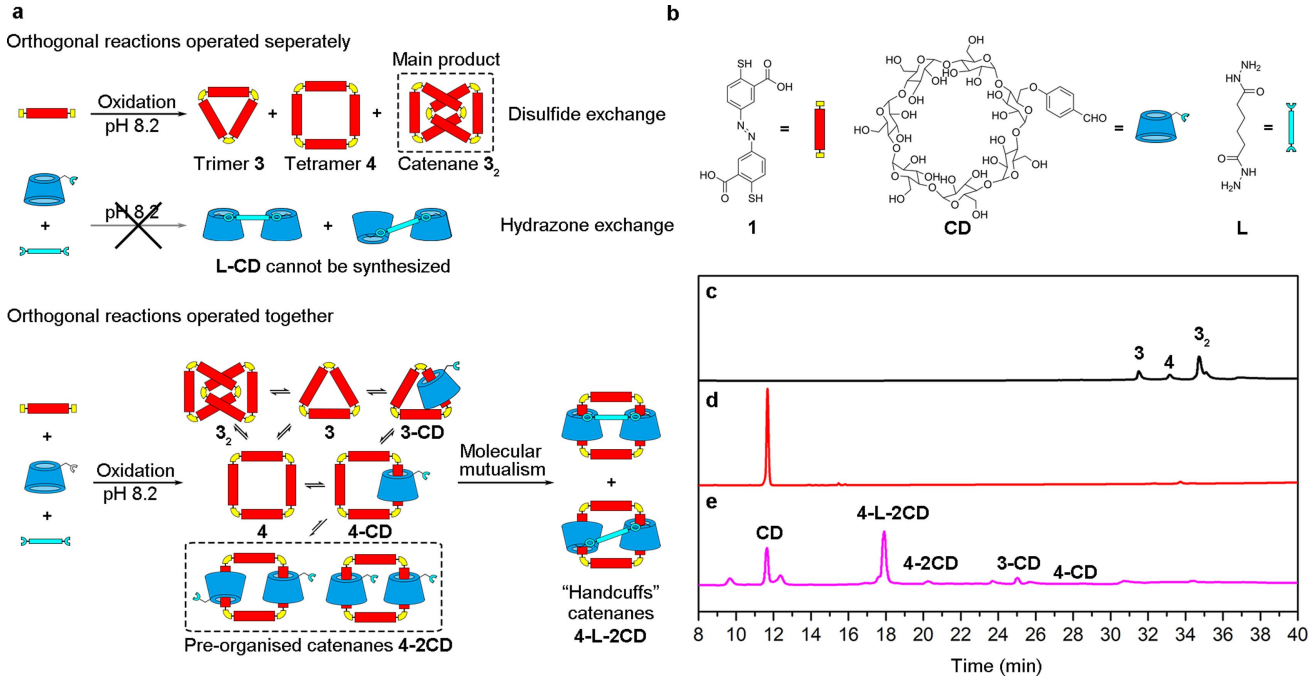

Figure 1. (a) Schematic presentation of a pair of orthogonal reactions operated separately and together; (b) Molecular structures of building blocks **1**, **CD**, and **L**; HPLC-MS analysis of DCLs made from building blocks (c) 1.5 mM of **1**, (d) 1.5 mM of **CD** and **L**, and (e) 1.5 mM of **1**, **CD** and **L** in aqueous borate buffer (50 mM, pH 8.2). The HPLC spectra were monitored at wavelength 254 nm.

coevolution" for the origin of life. We envision that the validated concept of mutualistic synthesis may lead to new strategies to explore functional composite materials shortly and de novo life later.

The pair of orthogonal dynamic covalent reactions chosen to make the DCLs were the classical disulfide and hydrazone exchange, as the disulfide exchange is active in water at pH 8.2 while the hydrazone exchange is inert at the same experimental condition. The disulfide DCL was prepared from an azobenzene-derived dithiol building block **1** (1.5 mM) in an aqueous solution at pH 8.2. The two thiol groups of building block **1** could be oxidized into disulfide bonds as the linkages of macrocyclic molecules at room temperature in the air. The exchange reaction continued when thiols remained in the reaction. As our previous report,[10] once all the thiols were fully oxidized, the high performance liquid chromatography-mass spectrometry (HPLC-MS) analysis revealed that the dominant product was a catenane $\mathbf{3_2}$ interlocked by two trimeric macrocycles **3**, and two minor species were the trimer **3** and the tetramer **4** (Figure 1c). Parallelly, the hydrazone DCL was made from a β-cyclodextrin derived aldehyde building block **CD** (1.5 mM) and an adipic dihydrazide building block **L** (1.5 mM) in aqueous solution at the same experimental condition (Figure 1d). As expected, no products were detected, since the hydrazone formation is thermodynamically and kinetically unfavorable in water at the slightly basic pH.[11]

However, when the two DCLs were performed together in the same solution (pH 8.2) with the same concentration as they were performed alone, HPLC analysis showed only one new product peak and the molecular weight of the peak was the sum of that of the disulfide tetramer **4** and that of the linear hydrazone **L-2CD** dehydrated by one molecule of **L** and two molecules of **CD** (Figure 1e and S1). Considering that the azobenzene unit has the tendency of threading through the well-matchable cavity of the β-CD moiety in water, we inferred that the new product peak should correspond to a "handcuffs" catenane **4-L-2CD** interlocked by hybrid species, the disulfide **4** and a linear hydrazone **L-2CD**. To identify the number of **CD** interlocked with **4**, we added excessive hydroxylamine in the library to break up **L-2CD**. The HPLC-MS analysis showed that the residual catenane was **4-2CD-OH**, suggesting that two **CD** moieties were interlocked with **4** in "handcuffs" **4-L-2CD** structure (Figures S5–6). The neat production showed that the minor species **4** and **L-2CD** from the respective DCL dominated the complex chemical system when the two libraries were performed together, demonstrating that the **4** and **L-2CD** were a pair of mutualistic molecules.

Such a remarkable co-amplification of **4** and **L-2CD** should be mutually benefited from their binding. If our speculation of the "handcuffs" catenane formation was correct, the interlocked structure should remain stable during the purification process from the reaction mixture. Indeed, we could isolate the both of **4-2CD** and **4-L-2CD** as a mixture of isomers, including the parallel (head-to-head) and anti-parallel (head-to-tail) conformation[10,12] using preparative HPLC (Figures S7–8), which were characterized by a number of ^{1}H NMR spectroscopic experiments (Figures 2b and S9–17). A diffusion ordered spectroscopy (DOSY) spectrum showed that both **4** and **L-2CD** had the same

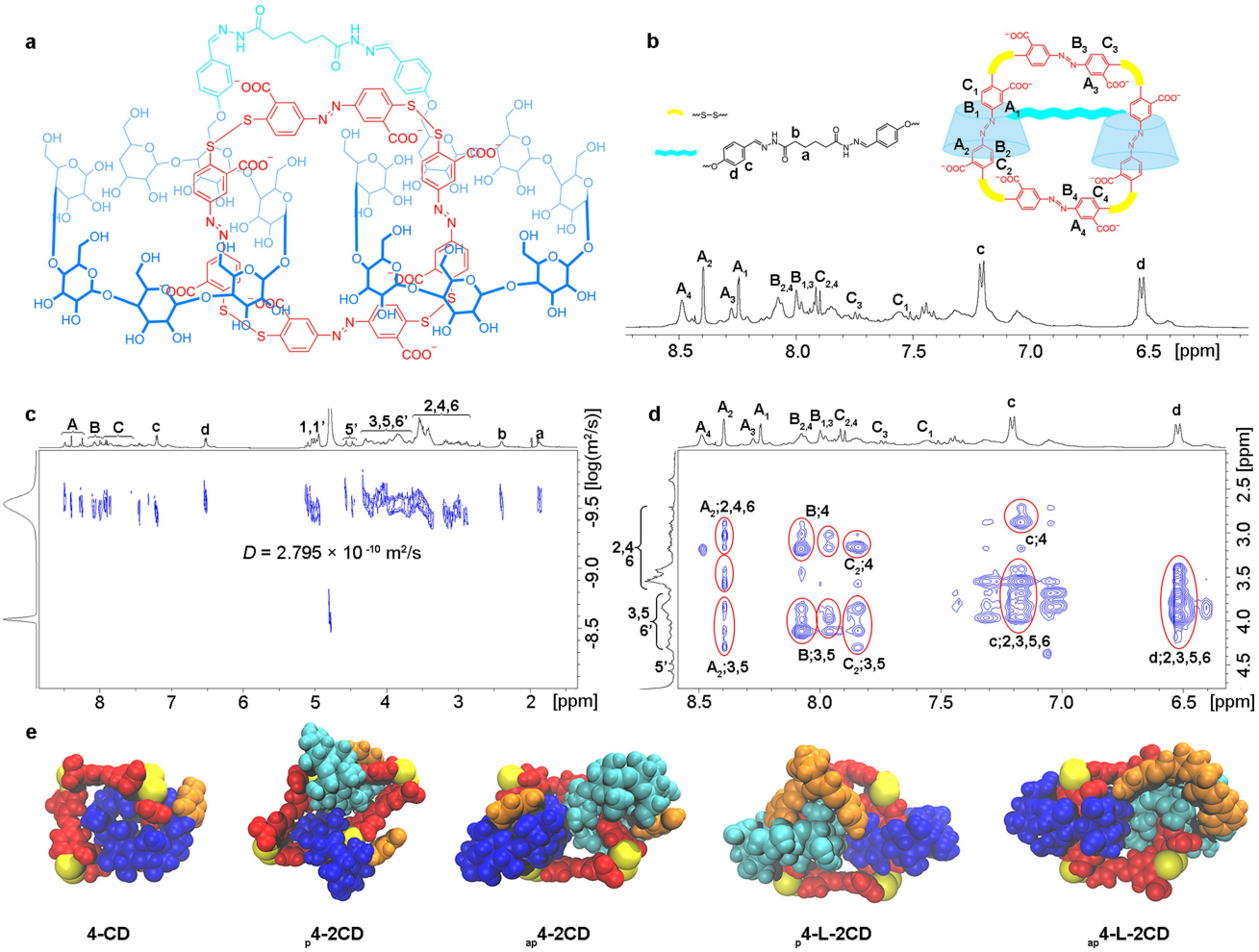

Figure 2. (a) Molecular structure of **4-L-2CD** in parallel orientation; (b) ^{1}H NMR spectra of **4-L-2CD**. (D_2O, pD = 8.2, 500 MHz, 298 K); (c) The 2D DOSY spectra of **4-L-2CD**. (D_2O, pD = 8.2, 500 MHz, 298 K); (d) Part of 2D ^{1}H-^{1}H NOESY spectra of **4-L-2CD**. (D_2O, pD = 8.2, 500 MHz, 298 K); (e) Representative structures of catenanes obtained using molecular dynamics. Red: azobenzene part; yellow: disulfide bond; orange: adipic dihydrazone linker; blue and cyan: **CD** part.

diffusion rate constant at $2.795\times10^{-10}\,m^2s^{-1}$ (Figure 2c), which confirmed the supramolecular complexation of the two species. The ^{1}H NMR spectrum of **4-L-2CD** showed four sets of signals (A, B, and C) for tetramer **4**, as the local symmetry of azobenzene was affected by the interlocked **L-2CD** (Figure 2b and S15).[13] The presence of only one set of phenyl signals of **L-2CD** at 7.21 and 6.51 ppm was consistent with a symmetrical structure, indicating that the parallel conformation **$_p$4-L-2CD** was the dominant product in the mixture (Figure 2a).[13e] The peaks at 8.24 and 8.39 ppm were assigned to the protons A_1 and A_2 of azobenzene units included inside the **CD**, as they experienced varying degrees of shielding from **CD** cavity. Based on the Nuclear Overhauser effect spectroscopy (NOESY) (Figure 2d), NOE signals were observed between A_2-3,5,6, B-3,4,5, and C_2-3,4,6, confirming the part of tetramer **4** was mechanically encapsulated in **CD** cavity in **4-L-2CD**. On the other hand, the ^{1}H NMR spectrum of **4-2CD** showed two sets of phenyl signals of **CD** at 7.44 and 6.59 ppm, indicating two possible isomers, with either a head-to-head or head-to-tail orientation of two **CD**s, have been obtained (Figure S10). Compared with catenane **4-2CD**, protons c and d on phenyl moieties of **4-L-2CD** were shifted upfield (from δ = 7.44 to 7.21 ppm for c and from δ = 6.59 to 6.51 ppm for d). However, no NOE signal appeared between proton a and b on the linker **L** and **CD**, indicating **L** was far away from the **CD**. Besides, some small peaks appeared at 7.05 and 6.41 ppm, which had NOE signals with **CD** cavity. These should be attributed to the protons of phenyl groups in anti-parallel conformation **$_{ap}$4-L-2CD**.

Complementary to the experimental approach, further insights into **4-L-2CD** structure were obtained at the atomistic level through molecular dynamic (MD) simulations undertaken within the Gromacs 5.0.[14] The **4-L-2CD** components were described with General Amber Force Field (GAFF) parameters[15] and using MMFF94 charges.[16] The remaining classic force field parameters and simulation details have been given in the Supporting Information Section 5. The starting parallel conformation **$_p$4-L-2CD** was immersed in cubic boxes composed of water molecules. We

simulated $_{p}$**4-L-2CD** involved in equilibrium for 20 ns. Through most of MD runs, the shortest distance between protons A_2 of **4** inside the **CD** cavity to protons 3, 5, and 6 of **CD** were less than 6 Å separately, and the distances between protons c and d on phenyl moieties to the protons 5 and 6 of the **CD** were less than 5 Å periodically (Figure S18). These distances were consistent with the NOE signals (A_2-3,5,6; c-3,5,6; d-3,5,6) in NOESY spectroscopy. For $_{ap}$**4-L-2CD**, the distance between A_2 to proton 6 of **CD** was more than 10 Å through the run, while the distances between protons c and d of phenyl groups to 5 and 6 of **CD** were less than 5 Å for part of the time (Figure S19). These results confirm that the small peaks at 7.05 and 6.41 ppm, which had NOE signals with **CD**, attributed to protons c and d of the anti-parallel conformation $_{ap}$**4-L-2CD**.

To investigate why the "handcuffs" catenane **4-L-2CD** was the most favorable catenane in this system, we simulated the systems involved in the equilibrium leading to the formation of catenanes containing **4** and **CD** (**4-CD**, **4-2CD**, and **4-L-2CD**), and calculated the change of free energy of binding (ΔG). Applying Multistate Bennett acceptance ratio (MBAR)[17] method, we got the following numerical data (Table S1) for the binding energy for the formation of catenanes. The docking results showed that **4-L-2CD** had a higher binding energy value than the other catenanes, indicating the highest stability of **4-L-2CD** in the library. The binding energy of $_{p}$**4-L-2CD** and $_{ap}$**4-L-2CD** was determined to be -66.40 ± 0.20 and -57.24 ± 0.23 kcal mol^{-1}, respectively. The lowest energy conformation for **4-L-2CD** was the parallel conformation $_{p}$**4-L-2CD**, which was in agreement with the dominant product in ^{1}H NMR spectra obtained in solution.

Then, we calculated the change of solvent-accessible surface area (ΔSASA) of catenanes in the systems. After an initial equilibration phase, all the systems trended to stable trajectories, and the visual inspection of equilibrated trajectories revealed that the systems towards the conformations minimizing exposed hydrophobic surfaces in all cases (Figure 2e). The results showed that the values of SASA in all the systems decreased as the catenanes formed, which followed the same trend as the binding energy. When **4** was associated with **CD** in solution, the SASA of the hydrophobic regions of both **4** and **CD** tended to minimize, driving the decrease of free energy. In accordance with the expected, parallel conformation $_{p}$**4-L-2CD**, which experienced the greatest reduction in SASA, had the lowest binding energy.[18] Hence, the most stable catenane $_{p}$**4-L-2CD** was formed in the library.

Once we had a better structural understanding of the "handcuffs" catenane **4-L-2CD**, we moved forward to unravel the mechanism behind the mutualistic synthesis of its two components, **4** and **L-2CD**. As the hydrazone formation is kinetically unfavorable in water at pH 8.2 in general and it could not be catalyzed by the carboxylic acids of a control thiol building block (see Figure S20), the synthesis of the **L-2CD** should be catalyzed by the pre-organized catenane structures consisting of the tetramer **4** and the aldehyde **CD**. Thus, we first prepared the control group (**1**+**CD**) as a starting point to investigate the complex equilibrium of the system (see Supporting Information Section 7). A simplest model that was able to produce a good fit in the presence of a series of catenanes was established in Figure S24. The strong amplification of the pre-organized catenane **4-2CD** was reflected in the high affinity of the host to the guest, with formation constants of around 9.55×10^{2} M^{-1} and 1.55×10^{4} M^{-1} upon binding of the first and the second **CD**, respectively. To verify the calculated formation constants in the system, we fitted the dataset in *DCLFit*.[19] The results showed that the calculated and fitted data were essentially consistent (Figure S25, Table 1). The formation constant for the first binding of **CD** to the tetramer **4** ($K_{4\text{-CD}}$), had the same order of magnitude as the binding constant of **CD** to monomer **1** obtained by UV titration (see Supporting Information Section 8). However, the formation constant for incorporating the second **CD** to yield **4-2CD** was an order magnitude larger, implying that the tetramer **4** had the cavity suitable for the interaction with two **CD**s to form catenane **4-2CD**, while the trimer **3** cavity was large enough to fit only one **CD**. These results proved that in the library (**1**+**CD**), catenane **4-2CD** was a thermodynamically favorable product, which may become the prerequisite to catalyst hydrazone formation in the library composed of **1**, **CD**, and **L** referred to as library (**1**+**CD**+**L**).

Then, we investigated the hydrazone formation by preparing a series of DCLs from building block **1**, hydrazide **L**, and aldehyde **CD** with various concentrations, and the model was designed to fit the library distributions (Figure 3).

Table 1: Formation constants of catenanes in DCLs.[a]

	Log K_a[a]			
	4-L-2CD	**4-2CD**	**4-CD**	**3-CD**
1+**CD**[b]	/	4.19±0.16	2.98±0.25	4.06±0.16
Fitting[c]	/	4.11±0.09	3.01±0.30	4.02±0.10
1+**CD**+**L**[b]	/	4.07±0.11	3.24±0.24	3.79±0.28
Fitting[c]	1.16±0.02	4.00±0.12	3.20±0.04	3.92±0.08

[a] The corresponding binding constant K are in M^{-1}. [b] Formation constants are calculated from Equation S2. [c] Formation constants are fitted by *DCLFit* software.

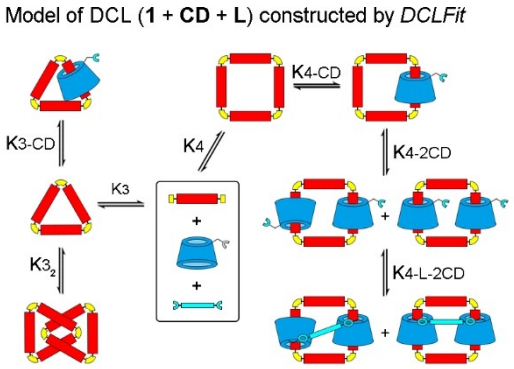

Figure 3. Model of the library distributions obtained for different concentrations of **CD** in the experimental group (**1**+**CD**+**L**) constructed by *DCLFit*; Stoichiometries omitted for clarity.

The HPLC-MS analysis revealed that "handcuffs" catenanes **4-L-2CD** became the dominant product in the libraries (**1**+**L**+**CD**), while catenanes **4-2CD** became the main sacrifice for their production. While **L-2CD** could not be synthesized directly in the libraries, the formation constant of **4-L-2CD** obtained in *DCLFit* was $14.48 \pm 0.67\ M^{-1}$ (Figure S26, Table 1). These results demonstrated that the pre-organized catenane **4-2CD** structures could effectively catalyze the hydrazone formation (**L**+2**CD**→**L-2CD**) at pH 8.2, while the formation of **L-2CD** made tetramer **4** stable through the formation of **4-L-2CD** in DCL. Hence, **4** and **L-2CD** were a pair of mutualistic molecules, leading to the high yield of "handcuffs" catenane **4-L-2CD**.

Based on the previous experiments, we have demonstrated that **4-L-2CD** was a thermodynamically stable product, produced by the two orthogonal reversible chemical reactions. Subsequently, we studied the kinetics to understand the mutualistic synthesis better. First, the compositional change of a DCL prepared from only the building block **1** (1.5 mM) in borate buffer (50 mM, pH 8.2) was monitored over time using HPLC. A rapid increase in the amount of catenane $\mathbf{3_2}$ (around 76 %) was followed by a slight decrease after 36 h, which coincided with the gradual concentration growth of **3**, probably attributed to the breakage of $\mathbf{3_2}$ (Figure 4a). In the DCL starting from an equimolar of solution **1** and **CD** (1.5 mM), the species **4-CD** formed rapidly in 12 h, followed by decreasing to 1.6 %, while **4-2CD** became the dominant species after 24 h (Figure 4b). The phenomenon should be attributed to the positively cooperative binding in the formation of **4-2CD**. This is supported by the fact that the association affinity observed in the secondary binding of **CD** with **4-CD**, crucial for the formation of **4-2CD**, was an order of magnitude higher than that observed in the initial binding of **CD** for the formation of **4-CD**. Then, in the DCL made from **1**, **L**, and **CD** (1.5 mM), once **4-L-CD** appeared, it grew dramatically over 50 % in 36 h at the expense of other species (Figure 4c).

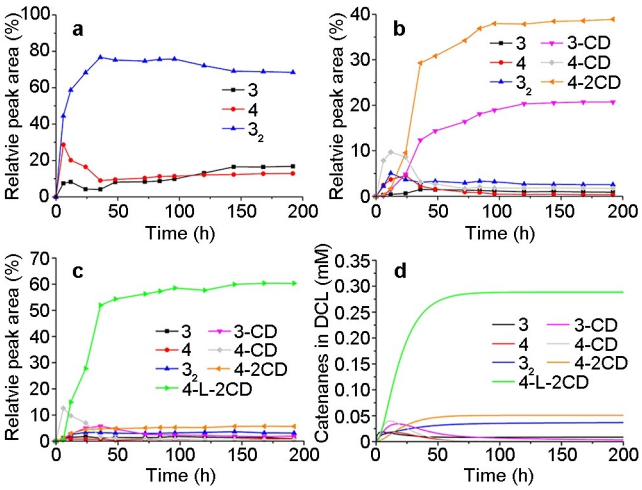

Figure 4. Kinetics study of catenane formation in DCLs of (a) 1.5 mM of **1**; (b) 1.5 mM of **1** and **CD**; (c) 1.5 mM of **1**, **CD**, and **L**; (d) Kinetic modelling results of the catenanes in DCL containing 1.5 mM of **1**, **CD**, and **L**.

We constructed a simplified mass-action-kinetics model to show that the mutualistic relation of **4** and **L-2CD** can indeed be a result of three building blocks (**1**, **CD**, and **L**) that had influences on each other in DCL (Figure S32). First, we determined the majority of the involved rate constants and reaction orders experimentally, including the rates of thiol oxidation, thiol-disulfide exchange, breakage of catenane, and hydrazone formation (see Supporting Information Section 9). These experimentally measured data were used to parameterize a kinetic model,[9j,20] with which we analyzed the reactions through pathways. The experimental kinetic analysis of hydrazone formation showed that the reaction **4-2CD**+**L**→**4-L-2CD** in solution occurred rapidly and the rate constant of hydrazone formation was measured as $k = 12.81\ M^{-1}h^{-1}$, which was close to the calculated value $14.95\ M^{-1}h^{-1}$ (Tables S5–6, Figure 4d) using the kinetic model for the hybrid library. The high reaction rate of the hydrazone formation offered a potentially fast competing pathway to equilibrium, suggesting that the thermodynamic stable **4-2CD** from a disulfide library acted as the transition state to catalyze the hydrazone formation.

In conclusion, we have demonstrated the concept of mutualistic synthesis involving species from orthogonal reversible chemical reactions. Facilitated by supramolecular interactions, we observed that when these reactions occurred concurrently in a single vial, two initially minor products became predominant. Specifically, a reactant from the inert reaction served as a template, selectively amplifying a minor library species from the active reaction. This process led to the formation of a thermodynamically stable catenane through noncovalent binding. This catenane, acting as a transition state, catalyzed the inert reaction between its associated reactant and the other freely present reactant in the solution. This interaction resulted in the dominant products of both reactions aiding each other's formation, demonstrating a mutualistic relationship. However, we also noted a limitation: the mutualistic species formed extremely stable catenane structures resembling "handcuffs", impeding their dissociation and reactivity in subsequent inert reaction cycles, thus limiting catalytic efficiency. We envision this challenge can be addressed by adjusting noncovalent affinities among species in new molecular systems to enable these species to cross-catalyze the orthogonal reactions more effectively.

Our findings highlight the potential of positive cooperativity in synthesizing species from both inert and active reactions, showing the feasible coevolution of mutualistic species from chemical reactions. This approach opens new avenues for seeking clues to support the hypothesis of "RNA-peptide coevolution" for the origin of life and exploiting the synthesis of minor products in chemical reactions more broadly. Furthermore, the ability of the mutualistic species to form supramolecular complexes paves the way for their co-self-assembly into nanosystems. This advancement holds significant promise for the synthesis of functional composite materials with novel synergic properties.

Acknowledgements

We are grateful for the financial support from the Sigrid Jusélius Foundation (senior researcher fellowship for J.L.), the Academy of Finland (Decision No.318524, project funding for J.L.), the Finnish Cultural Foundation (PhD fellowship for Y.L.) and China Scholarship Council (PhD scholarship for J.Y. and X.W.). We thank Turku Centre for Chemical and Molecular Analytics at the University of Turku for providing NMR and LC-MS technology.

Conflict of Interest

The authors declare no conflict of interest.

Data Availability Statement

The data that support the findings of this study are available from the corresponding author upon reasonable request.

Keywords: Dynamic combinatorial chemistry · Catenanes · Supramolecular chemistry · Systems chemistry · Hydrazone

[1] a) J. L. Bronstein, in *Mutualism* (Ed.: J. L. Bronstein), Oxford Press, Oxford, **2015**, pp. 3–19; b) A. E. Douglas, in *Mutualism* (Ed.: J. L. Bronstein), Oxford Press, Oxford, **2015**, pp. 20–34; c) M. W. Schwartz, J. D. Hoeksema, *Ecology* **1998**, *79*, 1029–1038.

[2] a) B. Wang, Y. L. Qiu, *Mycorrhiza* **2006**, *16*, 299–363; b) L. Lanfranco, P. Bonfante, A. Genre, *Microbiol. Spectr.* **2016**, *4*, 10.

[3] D. W. Yu, *Biol. J. Linn. Soc.* **2001**, *72*, 529–546.

[4] J. N. Holland, J. L. Bronstein, in *Encyclopedia of Ecology* (Eds.: S. E. Jørgensen, B. D. Fath), Academic Press, Oxford, **2008**, pp. 2485–2491.

[5] V. I. Ogharanduku, A. T. Tinuoye, in *Handbook of Research on the Impact of Culture in Conflict Prevention and Peacebuilding*, IGI Global, **2020**, pp. 177–198.

[6] K. A. Carson, *Studies in mutualist political economy*, BookSurge, **2007**.

[7] a) M. Frenkel-Pinter, J. W. Haynes, A. M. Mohyeldin, M. C, A. B. Sargon, A. S. Petrov, R. Krishnamurthy, N. V. Hud, L. D. Williams, L. J. Leman, *Nat. Commun.* **2020**, *11*, 3137; b) R. M. Turk, N. V. Chumachenko, M. Yarus, *Proc. Nat. Acad. Sci.* **2010**, *107*, 4585–4589; c) S. Tagami, J. Attwater, P. Holliger, *Nat. Chem.* **2017**, *9*, 325–332.

[8] a) J. M. Lehn, A. V. Eliseev, *Science* **2001**, *291*, 2331–2332; b) P. T. Corbett, J. Leclaire, L. Vial, K. R. West, J. L. Wietor, J. K. M. Sanders, S. Otto, *Chem. Rev.* **2006**, *106*, 3652–3711; c) F. B. L. Cougnon, H. Y. Au-Yeung, G. D. Pantos, J. K. M. Sanders, *J. Am. Chem. Soc.* **2011**, *133*, 3198–3207; d) F. B. L. Cougnon, J. K. M. Sanders, *Acc. Chem. Res.* **2012**, *45*, 2211–2221; e) J. Li, P. Nowak, S. Otto, *J. Am. Chem. Soc.* **2013**, *135*, 9222–9239; f) A. G. Orrillo, R. L. E. Furlan, *Angew. Chem. Int. Ed.* **2022**, *61*, e202201168.

[9] a) P. W. J. M. Frederix, J. Idé, Y. Altay, G. Schaeffer, M. Surin, D. Beljonne, A. S. Bondarenko, T. L. C. Jansen, S. Otto, S. J. Marrink, *ACS Nano* **2017**, *11*, 7858–7868; b) A. G. Orrillo, A. La-Venia, A. M. Escalante, R. L. E. Furlan, *Chem. Eur. J.* **2018**, *24*, 3141–3146; c) M. Dumartin, J. Septavaux, M. Donnier-Maréchal, E. Jeamet, E. Dumont, F. Perret, L. Vial, J. Leclaire, *Chem. Sci.* **2020**, *11*, 8151–8156; d) Z. Yang, J.-M. Lehn, *J. Am. Chem. Soc.* **2020**, *142*, 15137–15145; e) T.-M. Gianga, E. Audibert, A. Trandafir, G. Kociok-Köhn, G. D. Pantoş, *Chem. Sci.* **2020**, *11*, 9685–9690; f) D. Komáromy, T. Tiemersma-Wegman, J. Kemmink, G. Portale, P. R. Adamski, A. Blokhuis, F. S. Aalbers, I. Marić, G. M. Santiago, J. Ottelé, A. Sood, V. Saggiomo, B. Liu, P. van der Meulen, S. Otto, *Chem* **2021**, *7*, 1933–1951; g) R. Gu, J.-M. Lehn, *J. Am. Chem. Soc.* **2021**, *143*, 14136–14146; h) E. E. Harrison, B. A. Carpenter, L. E. St. Louis, A. G. Mullins, M. L. Waters, *J. Am. Chem. Soc.* **2021**, *143*, 14845–14854; i) O. Borodin, Y. Shchukin, C. C. Robertson, S. Richter, M. von Delius, *J. Am. Chem. Soc.* **2021**, *143*, 16448–16457; j) S. Yang, G. Schaeffer, E. Mattia, O. Markovitch, K. Liu, A. S. Hussain, J. Ottelé, A. Sood, S. Otto, *Angew. Chem. Int. Ed.* **2021**, *60*, 11344–11349; k) G. Schaeffer, M. J. Eleveld, J. Ottelé, P. C. Kroon, P. W. J. M. Frederix, S. Yang, S. Otto, *J. Am. Chem. Soc.* **2022**, *144*, 6291–6297; l) Y. Jin, P. K. Mandal, J. Wu, N. Böcher, I. Huc, S. Otto, *J. Am. Chem. Soc.* **2023**, *145*, 2822–2829; m) A. Erichsen, G. H. J. Peters, S. R. Beeren, *J. Am. Chem. Soc.* **2023**, *145*, 4882–4891.

[10] J. Li, P. Nowak, H. Fanlo-Virgós, S. Otto, *Chem. Sci.* **2014**, *5*, 4968–4974.

[11] a) J. Rayo, N. Amara, P. Krief, M. M. Meijler, *J. Am. Chem. Soc.* **2011**, *133*, 7469–7475; b) E. T. Kool, D.-H. Park, P. Crisalli, *J. Am. Chem. Soc.* **2013**, *135*, 17663–17666; c) A. Dirksen, P. E. Dawson, *Bioconjugate Chem.* **2008**, *19*, 2543–2548.

[12] D. Armspach, P. R. Ashton, C. P. Moore, N. Spencer, J. F. Stoddart, T. J. Wear, D. J. Williams, *Angew. Chem. Int. Ed.* **1993**, *32*, 854–858.

[13] a) D. Zhang, Y. Nie, M. L. Saha, Z. He, L. Jiang, Z. Zhou, P. J. Stang, *Inorg. Chem.* **2015**, *54*, 11807–11812; b) H. Onagi, B. Carrozzini, G. L. Cascarano, C. J. Easton, A. J. Edwards, S. F. Lincoln, A. D. Rae, *Chem. Eur. J.* **2003**, *9*, 5971–5977; c) A. W. H. Ng, Y. H. Leung, H. Y. Au-Yeung, *Org. Chem. Front.* **2021**, *8*, 2182–2189; d) C. W. Lim, S. Sakamoto, K. Yamaguchi, J.-I. Hong, *Org. Lett.* **2004**, *6*, 1079–1082; e) A. W. H. Ng, S. K.-M. Lai, C.-C. Yee, H. Y. Au-Yeung, *Angew. Chem. Int. Ed.* **2022**, *61*, e202110200.

[14] D. Van Der Spoel, E. Lindahl, B. Hess, G. Groenhof, A. E. Mark, H. J. C. Berendsen, *J. Comput. Chem.* **2005**, *26*, 1701–1718.

[15] J. Wang, R. M. Wolf, J. W. Caldwell, P. A. Kollman, D. A. Case, *J. Comput. Chem.* **2004**, *25*, 1157–1174.

[16] T. A. Halgren, *J. Comput. Chem.* **1996**, *17*, 490–519.

[17] M. R. Shirts, J. D. Chodera, *J. Chem. Phys.* **2008**, *129*.

[18] R. B. Hermann, *J. Phys. Chem.* **1972**, *76*, 2754–2759.

[19] a) R. F. Ludlow, J. Liu, H. Li, S. L. Roberts, J. K. M. Sanders, S. Otto, *Angew. Chem. Int. Ed.* **2007**, *46*, 5762–5764; b) R. A. R. Hunt, R. F. Ludlow, S. Otto, *Org. Lett.* **2009**, *11*, 5110–5113.

[20] B. Liu, J. Wu, M. Geerts, O. Markovitch, C. G. Pappas, K. Liu, S. Otto, *Angew. Chem. Int. Ed.* **2022**, *61*, e202117605.

[21] G. Bussi, D. Donadio, M. Parrinello, *J. Chem. Phys.* **2007**, *126*, 014101.

[22] H. J. C. Berendsen, J. P. M. Postma, W. F. van Gunsteren, A. DiNola, J. R. Haak, *J. Chem. Phys.* **1984**, *81*, 3684–3690.

[23] T. Darden, D. York, L. Pedersen, *J. Chem. Phys.* **1993**, *98*, 10089–10092.

[24] W. Humphrey, A. Dalke, K. Schulten, *J. Mol. Graphics* **1996**, *14*, 33–38.

Manuscript received: June 26, 2024
Accepted manuscript online: July 12, 2024
Version of record online: September 5, 2024